

Correction of Errors during the Manufacture by Computer Numerical Control (CNC) of Blades for an Axial Hydrokinetic Turbine

J. Graciano-Uribe^{1*}, J. Arbeláez¹, D. Hincapie¹, E. Chica², E. Torres²

¹Department of Mechatronic Engineering, Research Group - MATyER, Instituto Tecnológico Metropolitano, Medellín, 050034, COLOMBIA

²Department of Mechanical Engineering, Research Group Alternative Energy- (GEA), Universidad de Antioquia, Medellín, 050010, COLOMBIA

*Corresponding Author

DOI: <https://doi.org/10.30880/ijie.2022.14.01.002>

Received 21 September 2020; Accepted 15 February 2021; Available online 07 March 2022

Abstract: The design and manufacture of new systems for providing electric power to non-interconnected areas are challenges for engineering. There are several alternatives, including water or wind-power generation systems, where hydrokinetic turbines are highlighted. This work establishes the methodology, identification, and correction of errors generated during the manufacture by machining, using CAD/CAPP/CAM techniques, for an axial hydrokinetic turbine. During the manufacturing process, the generation of an error on the edges of the blades was identified, which was attributed to problems in the design of the model since the degrees of freedom of the manufacturing system used were not considered. For the manufacture of complex surfaces in the design of models, the most extreme points of the surfaces in contact must match the tangent edges to ensure that machining tools can reach them with the trajectories generated from the CAM.

Keywords: CAD/CAPP/CAM, adjustment of machining surfaces, degrees of freedom, control-machine

1. Introduction

Electric generation nowadays, access to electricity, transmission, distribution, and use of electricity, and the design of a range of related devices with power generation is a topic of interest for many researchers because these issues are essential for population life quality and natural resource use. The problem of accessing electricity varies across countries; however, in general, the use of electric power in places of difficult access or long distances from urban centers requires the building of thousands of kilometers of transmission and distribution lines for electricity, which brings huge installation and maintenance costs, and power losses in its transmission over long distances[1].

In Colombia, 52 % of the territory is not connected with the national electric grid [2]. These not connected zones are in remote areas under difficult geographical and natural conditions; they have 5 % of the population, which has motivated the country to promote the distributed generation of energy, mainly in isolated communities, reducing their dependence on large-scale infrastructure projects [3]. Most of the electricity supply in these areas is through diesel generators; however, their use has been limited due to high levels of pollution, cost, and difficulty in transport and storage of fuels. Most of these areas have the following characteristics: low population density, low payment capacity, unsatisfied basic needs, low consumption level, and high cost of energy service provision. These areas have adequate natural resources, which have not been exploited. Local energy generation is an important option to solve energy supply in non-interconnected areas of the national electricity grid. Currently, there are different mechanisms for distributed generation, such as photovoltaic systems, wind turbines, hydraulic systems without dams [4], and recently

the hydrokinetics turbines [5], [6]. At a global level, the United Nations established an installed capacity of 75 GW with small hydroelectric plants (PCH), with an additional potential of 173 GW to be developed in more than 150 countries, mainly in those countries located in the mountains [7].

Colombia counts with a hydroelectric generation capacity of 118 GW, considering 351 suitable rivers, of which the installed capacity is close to 10 GW; of these, a high percentage is generated by hydroelectric plants and by thermoelectric plants (gas, coal, and diesel principally). From the 351 rivers evaluated in the country, 5 % is ideal for small hydroelectric plants, equivalent to 5.9 GW [8]. Despite the attractiveness of these systems, characteristics such as the need for infrastructure, the reservoir, the dam, the pipelines for water conduction, the engine room, and the maintenance costs can be difficult to afford for the communities [9]. On the other hand, the hydrokinetic regimes manage to mitigate several of these difficulties because they are systems where the turbines are immersed in a current either in the sea or in a water source (river or artificial channel).

There are two types of turbines: horizontal axis and vertical axis turbines; among the latter, some vertical axis turbines design, such as the Savonius turbine, helical turbine (also known as Gorlov turbine), Darrieus turbine, and H-shaped Darrieus turbine, have been developed [10]. Vermaak *et al.* [11] carried out an excellent review of the types of hydrokinetic turbines, among which are highlighted those of horizontal axis with and without directed axial flow (ducted and unducted, respectively). This technology has been tested in different countries, being Brazil the closest place, where Van Els and Junior [12] described different microgeneration experiences. The ambitious design of an axial hydrokinetic turbine of 10 m of diameter was presented in this work. Simultaneously, Ismail *et al.* [13] presented the vertical hydrokinetic turbine design with a diameter of 1.0 m, where a generation of 1.6 kW was projected for the seven-blade system. Both experiences are focused on the electric generation in the Brazilian Amazon. In Colombia, Montoya *et al.* [14] evaluated the financial viability of implementing hydrokinetic systems, highlighting their feasibility, thanks to the great diversity of water sources available in the country, but showing their limited implementation as they are significantly dependent on the financial conditions of the market. This research contrasts with that of Kumar and Sarkar [15], who established that the costs mainly result from the turbine's size. In opposition, Muñoz *et al.* [16] established that the main source of costs lies in the design and manufacturing method. These authors underlined the importance of simulation, determined the optimal geometry, and manufactured the blades by computerized numerical control (CNC) as fundamental cost reduction elements.

Global manufacturing is a reality, driving companies to collaborate globally in product design, manufacturing, and assembly [17]. Since the third industrial revolution, automation has become a key technology in the industry, especially in CNC machines [18], [19]. The machine tool is one of the most critical manufacturing industry equipment, being the CNC controller is the key component to perform intelligent functions. This type of technology is essential in the manufacture of elements with complicated geometry. Due to the intricate combination of curves, the blades' geometry in these turbines is complex for the construction of a virtual and real model [20]. In the case of virtual models, free modeling tools were developed. However, for the building of real pieces, the technologies are still under development, trying to establish methodologies inspired by free modeling (freeform surfaces or sculptured surfaces) for their application in CNC manufacturing [21]. Among all the functions, the autonomous planning of intelligent processes is one of the essential functions to guarantee the machining quality. Currently, CNC machining centers employ G and M codes, focusing on the axes' movement, denying the process of the necessary information, such as part characteristics, tool properties, and optimized cutting parameters in a Computer Aided Process Planning (CAPP) system [22]. This information often relies on the operators' know-how to perform the optimization process, with inconsistent, inaccurate, and unreliable results. The standards for the Exchange of Product model data (STEP / ISO 10303) and Standard for the Exchange of Product model data for Numerical Control (STEP-NC / ISO 14649) allow encoding the complete machining information, as well as the exchange of data as the length of the design-machining chain [23], [24]. The STEP-NC data model provides much more comprehensive information and overcomes the G-M code's disadvantages, but still limited for autonomous process planning of the intelligent CNC controller [25].

However, this type of development is not yet available in most of the manufacturing industry. Considering the present technology, some difficulties in the manufacture of complex geometries are only observable during or at the end of the production process, is that most of them are corrected by the operators. It is recognized that some alternatives have been incorporated into NC systems. In machining, over-loading of spindle torque, cutting force, chatter, tool wear, and other metal cutting constraints are fundamental in generating the surface profile, mainly due to chatter and tool deflection induced by the cutting forces [26]. Several strategies have been designed to mitigate them; for example, the control of vibrations by modulating the spindle speed and optimizing the feed-rate using fuzzy control, reducing the spindle torque [27]. Likewise, it has been verified that the surface roughness is significantly affected by the feed rate, with an adverse effect of the cutting speed and little influence of the depth of cut [28], [29]. Furthermore, some difficulties in the manufacture of complex geometries are only observable during or at the end of the process. Any of these errors are related to the improper selection and deflection of the tools [30]–[32]; wrong interpolation or compensation of the tool trajectories [33], [34]; incorrect correction of tool weathering [35]; dynamic, static, and thermal expansion stress [36]; inadequate machining strategy [37]; and wrong definition of trajectories from the post-processing [38], [39]. The last one may seem unlikely since the trajectories are generated from the digital model, but they can occur as a consequence of the inadequate use of the tools, the machining sequence established for the

construction of the element, or the incompatibility of the virtual model and the degrees of freedom of the CNC machine. From the author’s knowledge, this type of problem has few references in the literature, seeing in many cases resolved intuitively by the technical staff, once the digital model arrives at the manufacturing workshop, leaving no room for reflection around the cause and the definitive correction. This research analyzes the origin and the way to correct compatibility problems in the construction of virtual models and the characteristics of the CNC machine during the construction of a prototype of blades for an axial hydrokinetic turbine using a 3+1-axis CNC machine.

2. Methods and Materials

Using the theories of the actuator disk and the blade element was designed a hydrokinetic turbine with a horizontal axis of 1.0 kW for a water velocity of 1.5 m/s, with a tip speed ratio (TSR) of 6.325, power coefficient of 0.4382, the efficiency of the transmission system of 70 %, and an angular speed of 12.009 rad/s [40], [41]. The rotor consists of a shaft with three blades of radius 0.79 m. The process of calculating the chord, thickness, and twist distribution of the blade section is described in [42].

In this research, prototypes of the blades for the hydrokinetic turbine of 1.0 kW were manufactured, at a scale of 4.5:30 and 1:1, using a methodology of integration CAD/CAPP/CAM systems. The sequence for the virtual model generation, the trajectories, and the manufacture of the blades are described. Once the code has been built, and the machining strategy has been defined for constructing the blades without errors, the same methodology is used to build a real-scale model.

2.1 Model Building

The process began with the CAD (Computer Aided Design) stage, where the blade was modeled from cross-sections with a parameterization of rotational shape and size, which allowed to reduce its cross-section. These sections rotate to the central axis as they move away from the origin (Fig. 1a). After having ten (10) cross-sections distributed along of blade length, they were connected by the surfaces, the first and the last cross-section were filled, and the other surfaces solidified to represent them as a volume. Finally, the extrusion of a parallelepiped was performed, which would be the base of the hydrokinetic turbine blade (Fig. 1b).

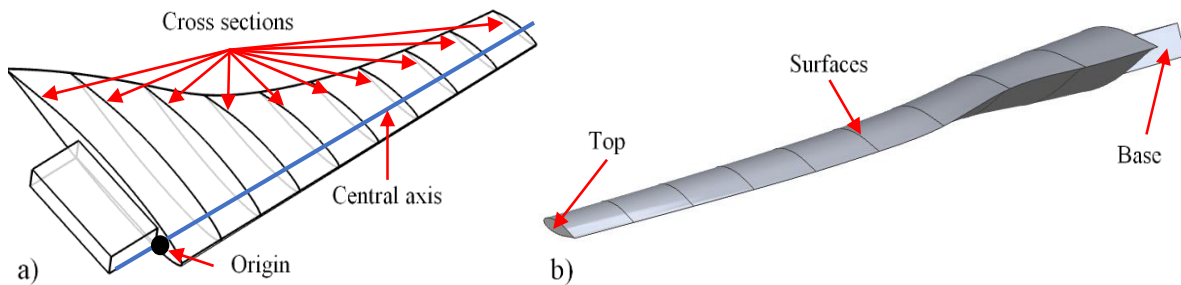


Fig. 1 - Scheme for the construction of the model of the hydrokinetic turbine blade [42]

2.2 Process Planning

Then, the CAPP (Computer Aided Process Planning) stage was developed, where the virtual models were manufactured in a Milltronics VM20 machining center, with four (4) indexed axes. The equipment has a Centurion 7 control, used in 3 + 1 mode. The prototypes were built using 7075-T6 aluminum alloy to withstand the stresses due to the drag and sustaining forces that originated during the operation and the stresses that appear during the machining process. Based on the previous statement, three cutting tools were selected: two ball milling cutters and one cylindrical milling tool, all of them with two flutes, ideal for machining aluminum alloys and materials with long chips, due to their large area of chip clearance and core diameter, which allows avoiding the dulling of the tool. Table 1 shows the parameters used for each of the described tools presented and the manufacturing material.

Table 1 - Cutting parameters of the two flutes cylindrical tools employed in the prototype construction

Material	Cutting speed (v_c , m/min)	Tool diameter (D_c , mm)	Feed per tooth (f_z , mm/tooth)
HSS	115	10	0.14
Carbide-Cermet	680	8	0.04
Carbide-Cermet	680	6	0.04

The rotation and cutting speeds are selected based on the equations: (1)-(3):

$$n = \frac{v_c * 1000}{\pi * D_{cap}} \text{ (rev/min)} \tag{1}$$

$$D_{cap} = \sqrt{D_c^2 - (D_c - 2 * a_p)^2} \tag{2}$$

$$v_f = n * Z_n * f_z \text{ (mm/min)} \tag{3}$$

Where n is the rotational speed (rev/min), Z_n is the number of teeth, D_{cap} is effective cutting diameter, and a_p is the cutting axial depth. Both f_z and v_c are data provided by the tool manufacturer. Additionally, a time correction v_f was used, only for round tools. The assembly of the system considered that the process would be carried out using the fourth axis rotary table of the machining center, where, for the fastening of the brick (raw material), a fixing clamp was manufactured in steel AISI-SAE 1020 of 2 inches of diameter (Fig. 2).

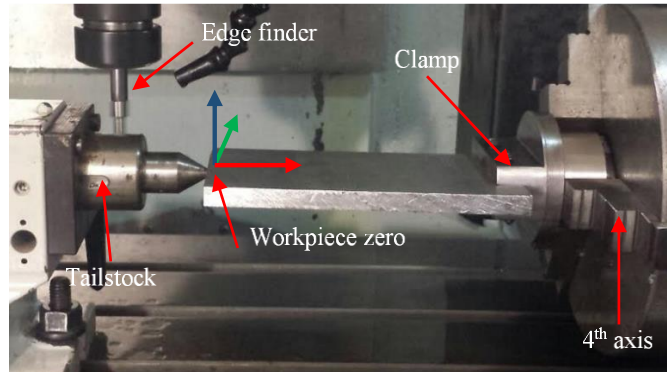


Fig. 2 - Mounting of the raw piece between the cup (4th axis) and the tailstock

The definition of the support -point/tailstock center- requires precision to guarantee the piece's proper machining. For this reason, after having the clamping device, the brick is assembled to the clamp to make the facing of the aluminum plate in the lathe, followed by drilling. Finally, the piece is mounted between the cup and the tailstock center in the CNC machining. The workpiece zero is in the interception of the tailstock center end and the solid aluminum blank, being located using an edge finder. For the X-axis, the tailstock was used, while for the Y-axis, the faced edge was employed; for the Z-axis, each one of the three tools was compensated.

2.3 Obtaining of Trajectory and the Code

The trajectories of tools were obtained in CAM. This stage declares the workpiece, the security guards (clamp and tailstock), the workpiece zero, and the security plane (Fig. 3); subsequently, the tree tools described in Table 1 are declared.

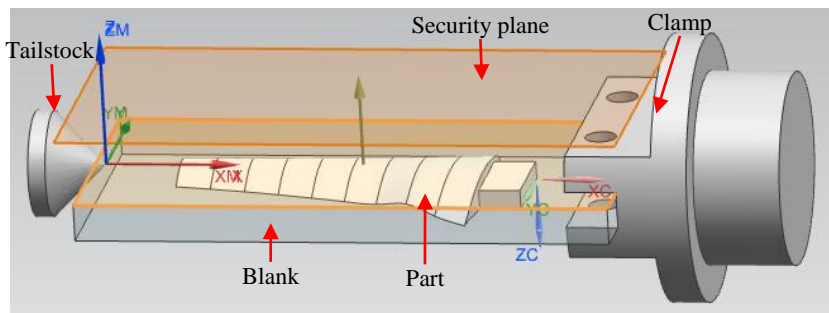


Fig. 3 - Definition of the geometries in the CAM model

After, the trajectory generation is conducted, which was divided into three phases: (1) roughing: with profiling and milling operations; (2) semi-finished: for the contour milling and (3) surface finishing and planning (Table 2). The G code was built with post-processing of the trajectories employing Siemens -NX 12.0 software.

Table 2 - Programed cutting parameters for the machining phases of the blade prototype

Parameters	Milling operation		
	Rough	Semi-finish	Finish
Feed rates (mm/min)	1100	2053	2737
Spindle speed (rpm)	3660	7000	7000
Cut depth (mm)	0.3	0.15	0.15
Part stock (mm)	1.0	0.15	0.0
Tool diameter(mm)	10	8.0	6.0

The roughing phase started with profiling to detach a significant portion of raw material without making a roughing to all the workpieces, as shown in Fig. 4.

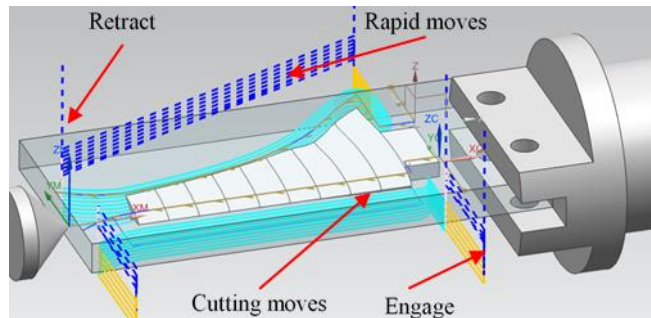


Fig. 4 - Manufacture trajectories in profiling, where NX12.0 ® represents with colors each section of the trajectory like: artic blue (cutting moves), blue (rapid moves, G0) and yellow (engage).

Then, the roughing in both sides of the turbine blade starts. In Fig. 5a-c, the simulation of the roughing and machining process in real-time, the semi-finish phase with the ball milling cutter of two teeth, and finishing with the ball milling cutter of two flutes are represented, respectively.

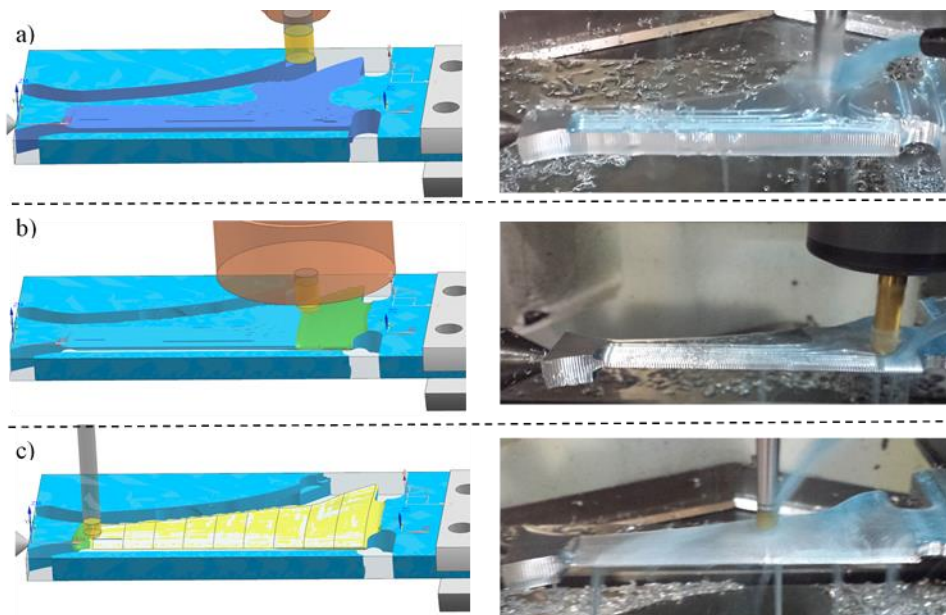


Fig. 5 - Manufacture trajectories during the profiling. a) rough, b) semi-finish and c) finish.

The post-processing is generated once the CAM design is completed. This step converts all linear entrance, machining, and exit trajectories, in G and M codes, with the header structure: activation of machine parameters, cutting moves with linear and circular interpolation, and program closing (shut down of the parameters).

2.4 Identification and Correction Errors

It is the final stage, where the different errors and their causes are identified to be appropriately corrected. The most relevant obey to mounting problems and rounding problems in the sharp edges of the blade. The corresponding results to the identification and solution of these problems are presented below.

2.5 Blade Manufacturing at Scale 1:1

The blades were manufactured with Proton MS (Castnylon+Molybdenum). Initially, due to the high cost of this material, the Proton blank's geometry was optimized to reduce wastes. For this purpose, a plate allowing two blades machining was taken as reference. For this reason, the first step was to separate the blank machining of each blade, as illustrated in Fig. 6a. Proton blank measures 1000 mm in length, 400 mm width, and 75 mm of thickness. This operation was carried out by designing a sketch to define the milling trajectory to cut the material. From this line, the profiling operation was concluded, as shown in Fig. 6b.

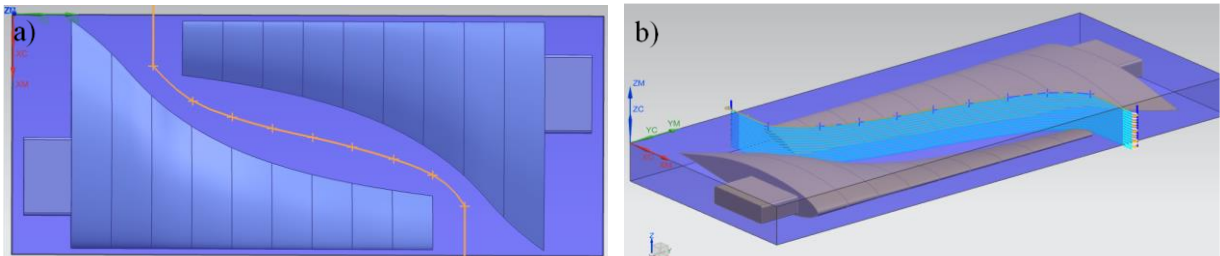


Fig. 6 - Processes for cutting the Proton blank. a) Assemble and sketch; b) simulation paths for cutting

Due to the bench's size limitations, the process was conducted with the fixed blank at the table of the machining center, without the use of the fourth axis. Each side was manufactured, the part was manually rotated. Three (3) steels records were fixed to the table before the machining to ensure zero workpiece during rotation, as represented in Fig. 7.

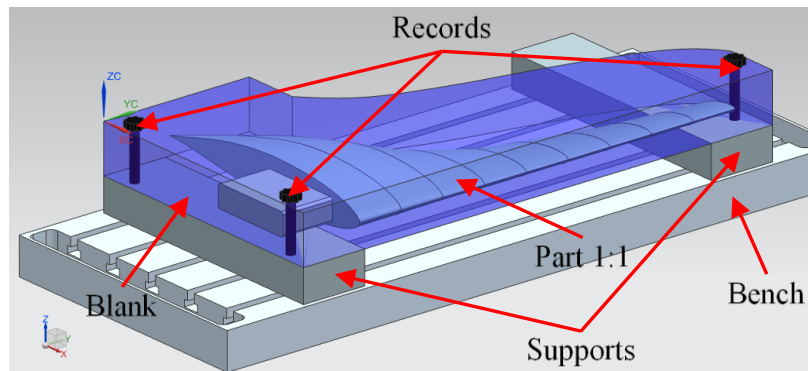


Fig. 7 - Mounting for machining of turbine blades in scale 1:1

Others replaced the tools used in the aluminum blades with a wider diameter for removing more material. The tools used were a cylindrical end mill of 1.0 in (25.4 mm) of diameter and two ball end mills tools with 12 mm and 8 mm of diameter. The cutting parameters were calculated based on Eq. (1)-(3) and are represented in Table 3.

Table 3 - Cutting parameters programed for the machining phases of the blade in scale 1:1

Parameters	Milling operation		
	Rough	Semi-finish	Finish
Feed rates (mm/min)	2300	1820	2053
Spindle speed (rpm)	4200	6540	7000
Cut depth (mm)	0.3	0.15	0.15
Part stock (mm)	1.0	0.2	0.0
Tool diameter(mm)	25.4	12.0	8.0

The rough mill phase starts with profiling operations to remove a big part of raw material (Fig. 8a), followed by the roughing (Fig. 8b) with parameters used in Table 3. The high depth of cut was used to reduce the machining. On the other hand, in this phase, a strategy for monitoring the roughing periphery based on machining geometric contour was used, where the entrances are from inside to out, intending to reduce the numbers of entrances and exits in comparison with the zig-zag machining strategy.

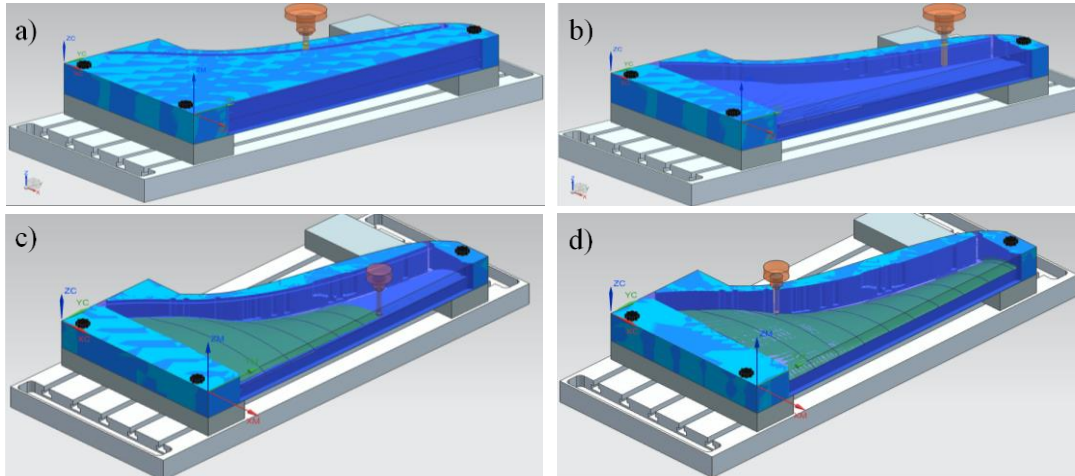


Fig. 8 - Machining process of the blade. a) Profiling; b) roughing; c) semi-finished; d) finished

The next step is the semi-finished (Fig. 8c); it is executed with a round tool of 12 mm and an oversize of 0.2 mm, an approximation to the blade's geometry and the removal of the steps generated in the roughing are achieved. In this phase, finer cutting conditions were used to prepare the material for the finished operation. Finally, the finished step is carried out (Fig. 8d), removing the excess previous process. Once the process was completed on surface 1 (Fig. 9a), the Proton blank was turned 180° for the machining of surface 2, using the same above-defined strategy. Finally, a profiling operation was performed to reach the blade's final shape (Fig. 9b). Once the system was manufactured, it was possible to determine the time employed for each operation in the final blade machining to establish its cost.

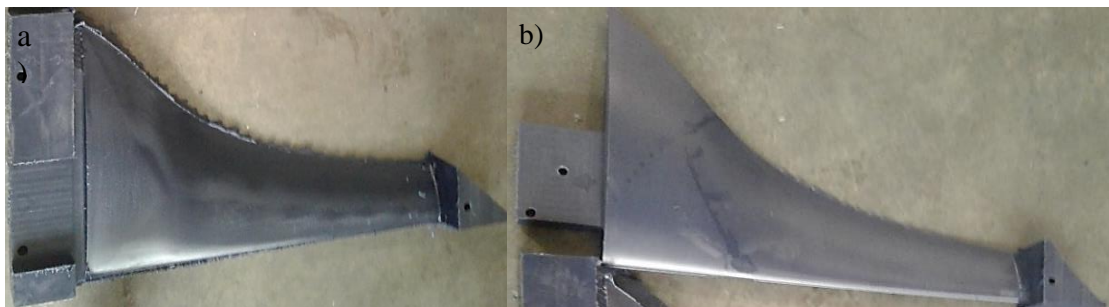


Fig. 9 - Blade manufacture on scale 1:1. a) The once surface 1 was finished; b) the once surface 2 was finished

3. Results and Discussion

Six blades were manufactured, three of them presented inconsistencies, which were corrected and allowed the manufacture of three blades with the right geometry for the prototype of an axial hydrokinetic turbine of 1 kW (Fig. 10). The fundamental errors during the manufacture are two types: (a) surfaces errors and (b) rounding errors, both shown in Figure 10a.

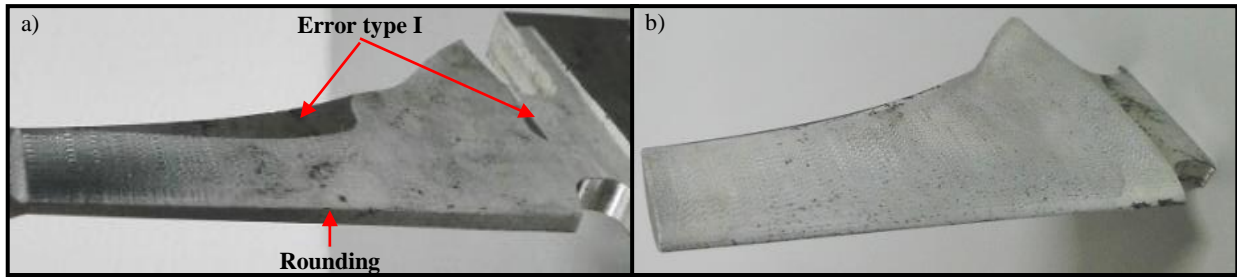


Fig. 10 - a) Blade with discrepancies in mechanized by the mounting; b) blade with the desired geometry

The surface errors refer to those faults where the tool does not produce an adequate material removal. Two defects observed in this process: (i) incorrect material removal, leaving the original surface of solid blank exposed, and (ii) incorrect material removal, generating small reliefs. In turn, error type (i) is due to the raw material's positioning problems and the zero location. It was corrected mechanizing the raw blank and the center hole for the tailstock mounting, described in section 2.2. Technicians typically correct these errors because it is a mounting problem of the machining system. To improve the precision in the manufacturing of complex surfaces and avoid type (ii) error generation, the thickness verification tool was used in the surface machining, as shown in Fig. 11a.

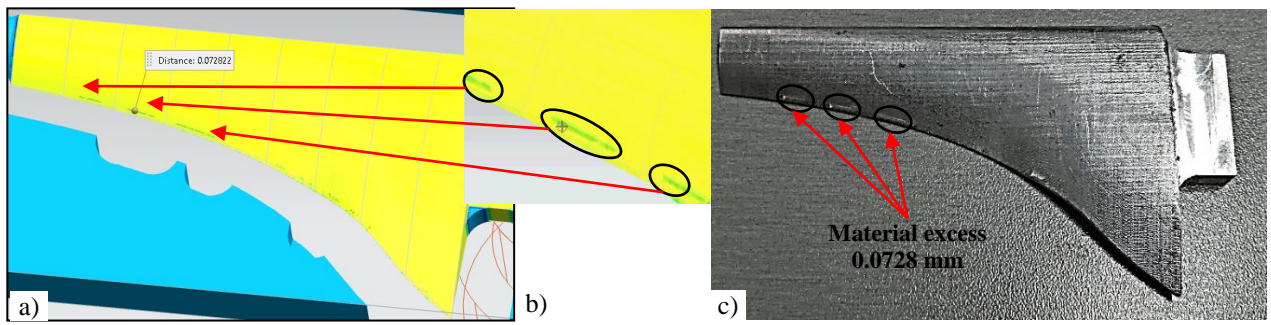


Fig. 11 - Superficial errors of mechanized type II. a) Registered by the simulator during the generation of trajectories; b) error detail; c) in one of the blades, material excess of 0.0728 mm

The above figure shows a material excess of 0.072 mm on one side of the blade. It is due to the generation of the slightest mistakes in the trajectories during superficial finishing. Figure 11b presents an example of errors in the blade prototype manufactured in aluminum, in which the same error observed in the simulation was identified, validating this tool as a suitable trajectory corrector. On the other hand, the defects due to rounding were originated in the trajectories generated in the G and M codes, during the post-processing of the trajectories, and movements in the contact points between the surfaces of the workpiece.

During the CAD process, a tool pad was generated, taking as reference the body surfaces and the grades of freedom of the device where the machining process was carried out. In this case, it corresponds to a system 3+1. This effect implies that each blade will be manufactured as follows: Surface I machining, fourth axis rotation, and surface II machining. Under this dynamic, the edges I and II of the blade were generated spontaneously because of both surfaces' material removal. The surfaces and the edges are shown in Fig. 12.

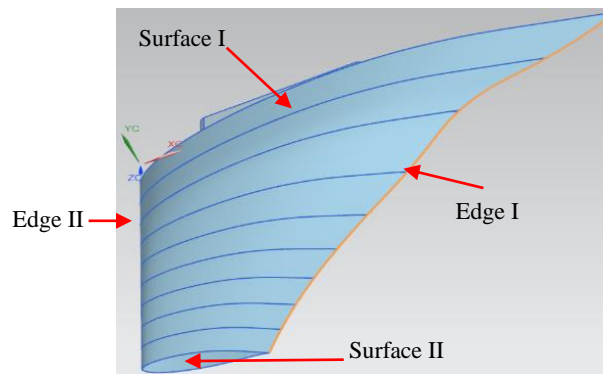


Fig. 12 - Blade edges generated as consequence of the surface contact of the element

However, during the material removal in each surface, sometimes the tools do not reach the edges, or those are surpassed, generating incorrect material removal with the subsequent dimension loss of the workpiece.

Dealing with identifying the error cause, a detailed review of the trajectories allows observing that it is never located tangent to it when the tool tries to reach edge II. This error is because the selected CAM method is surface milling, where the intercept of the two surfaces does not match with the most extreme or tangent edge, as shown in Fig. 13, with the arrow pointing to the mistake.

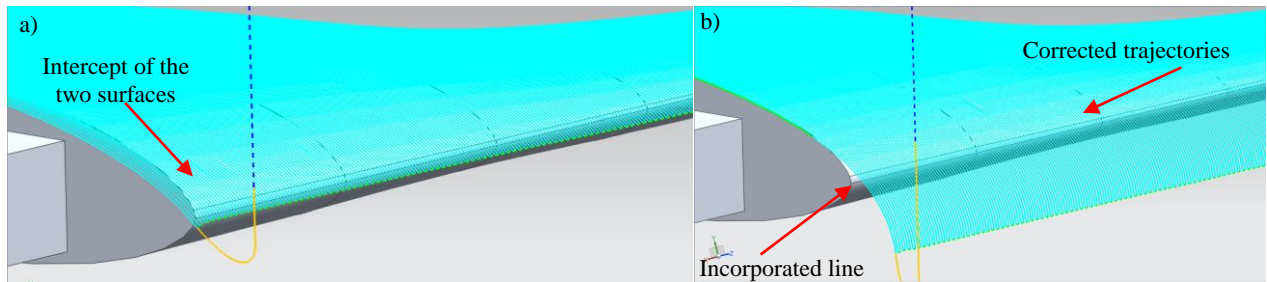


Fig. 13 - a) Initial model and generated trajectories; b) Modification of the simple model, incorporating a line in the blade edge

To correct this mistake, it can be used three strategies. (I) simple modifications of the model; (II) rebuilding the blade CAD model, where the surfaces I and II have as a contact the most extreme points of the pallet; (III) change CNC machining process, as a machining center with control and four or five indexed axes, to generate trajectories that allow reaching this point.

The strategy (I) was implemented, where an (XY) plane was generated in the blade center, in the plane, a line that divides the current surfaces was drawn, generating a meridional point or tangent to the edge (Fig. 13b). This line is identified by the CAM control, creating the tool's trajectory to reach this point. This strategy can be suitable in the manufacture of small objects because it is difficult to guarantee that the created line matches exactly the edge's further point.

Strategy II is more complicated because it involves rebuilding the element, but it is necessary not to make mistakes in creating surfaces with contact points different from the edge tangent ones. This strategy guarantees the manufacture of the elements without errors, not regarding the dimensions and characteristics of the CNC machine, since the further extreme of each surface matches with the edge tangent, the line that has been out lighted in Fig. 14.

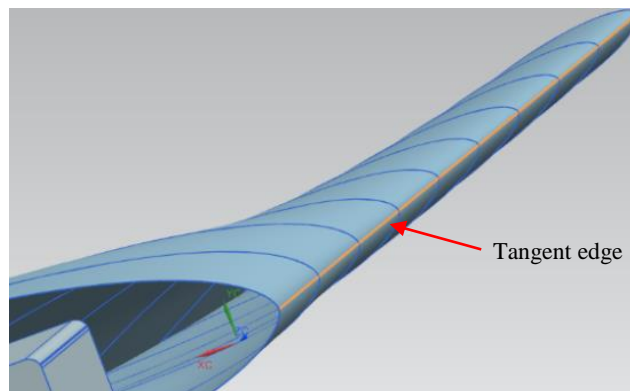


Fig. 14 - Blade CAM model redesign, guaranteeing the surfaces contact in the most extreme point

Notice that problem can be derived from the designer's lack of knowledge of dynamic characteristics of the CNC machine, this is the architecture or the grades of freedom of the machine -axes of the machine- and the programmable axes resulting of the generation of trajectories, which are due to the type of controller. The designer does not know how the tool's displacements are during the machining because it is wrongly considered that the CNC systems faithfully reproduce CAD models.

Strategy III considers the chance of manufacturing system. In this case, the change of a system 3+1 to other of a higher number of indexed grades of freedom allows that displacement and rotation of the piece simultaneously. Under this premise, the contact points are not relevant since in this machine, edges I and II will be reached easily, without creating a tangent edge. It leaves out the need for a designer to know the machining center's capacities, provided that

the system gets to generate complex trajectories -generated by the control system-while the architecture of the machine allows reproducing such displacements.

In Fig. 15a, the image of the turbine's prototype at a scale of 4.5:30, with the corrections previously described, is presented. Finally, the process that allows the construction of blades from the prototype was replicated for building the turbine at a 1:1 scale. In Fig. 15b-c, it can be observed the assembly of the blades with the rotor. The machining times of each blade, in a 1:1 scale, in each operation are presented in Table 4.

Table 4 - Operation time for the blade machining in a 1:1 scale

Operation	Time (h:min:s)
Roughing	4:44:08
Semi-finished	3:30:09
Finished	5:25:01
Mounting and preparation	0:35:02
Total	14:14:20

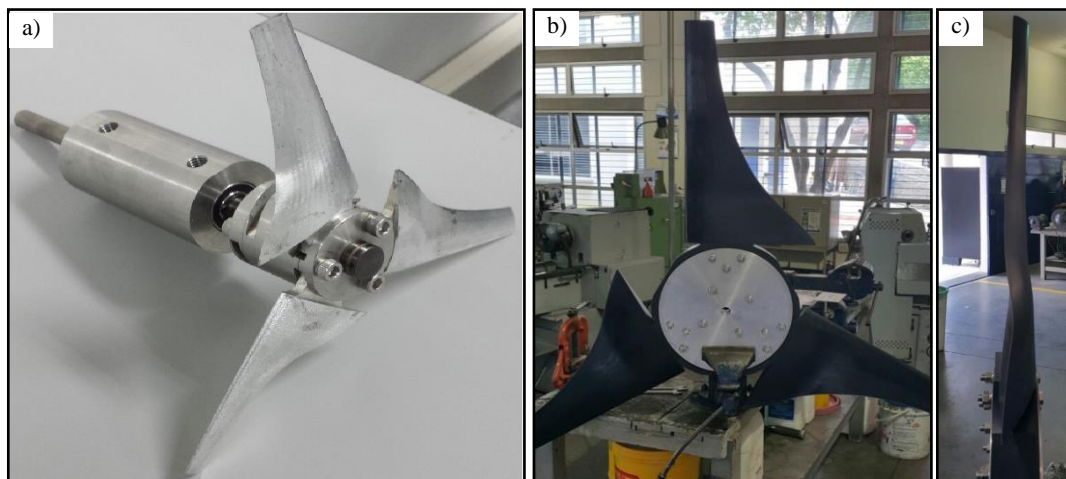


Fig. 15 - Images of the axial hydrokinetic turbine: a) model; b) turbine built at 1:1 scale; c) lateral view of the blade profile

Based on the times, it is possible to calculate the machining cost, calculated with an average cost of hour/machine of USD \$ 30, being the total value of USD \$427 for each blade. This value results in competitiveness, considering that this element's fabrication cost is generally the highest in compassion with other turbine elements. In this project, these costs were not significantly high compared to other elements (Table 5).

Table 4 - Operation time for the blade machining in a 1:1 scale

System	Cost (USD \$)
Turbine (blade, generator housing and supporting structure)	4000
Generator	912
Modular floating raft	1824
Total	6736

4. Conclusion

In this work, the blades of an axial hydrokinetic turbine of 1 kW were manufactured using a methodology of integration CAD/CAPP/CAM systems.

During the manufacturing, it was possible to identify two errors in the blades' edges due to problems in the model design without considering the grades of freedom of the employed manufacturing system. From the design, it is necessary to know the architecture of the manufacture system-freedom grades- and the indexed axis from the controller, to know if the edges in the contact surfaces, in any element, can be reached by the tool generated trajectories. In the design of complex surface models, the further points of the surfaces in contact must match with the tangent of the edge to guarantee that the machining tools can reach them with the generated trajectories in the CAM.

Surface machining errors were corrected employing the thickness verification tool that exposes the generation of small reliefs in the workpiece due to an inappropriate machining strategy.

Acknowledgement

The authors gratefully acknowledge the financial support provided by the Colombia Scientific Program within the framework of the call Ecosistema Científico (Contract No. FP44842-218-2018), Universidad de Antioquia (UdeA) and the Instituto Tecnológico Metropolitano (ITM).

References

- [1] G. Ardizzon, G. Cavazzini, and G. Pavesi, "A new generation of small hydro and pumped-hydro power plants: Advances and future challenges," *Renew. Sustain. Energy Rev.*, vol. 31, pp. 746–761, 2014, doi: 10.1016/j.rser.2013.12.043.
- [2] J. H. Flórez Acosta, D. Tobón Orozco, and G. A. Castillo Quintero, "¿Ha Sido Efectiva La Promoción De Soluciones Energéticas En Las Zonas No Interconectadas (ZNI) En Colombia?: Un Análisis de la Estructura Institucional," *Cuad. Adm. Adm.*, vol. 22, no. 38, pp. 219–245, 2009.
- [3] S. Ximena, C. Quintero, / Juan, D. M. Jiménez, J. David, and M. Jiménez, "Impacto de la generación distribuida en el sistema eléctrico de potencia colombiano: un enfoque dinámico The impact of distributed generation on the colombian electrical power system: a dynamic-system approach," *Tecnura*, vol. 17, no. 35, pp. 77–89, 2013.
- [4] D. K. Okot, "Review of small hydropower technology," *Renew. Sustain. Energy Rev.*, vol. 26, pp. 515–520, 2013, doi: 10.1016/j.rser.2013.05.006.
- [5] M. Anyi and B. Kirke, "Evaluation of small axial flow hydrokinetic turbines for remote communities," *Energy Sustain. Dev.*, vol. 14, no. 2, pp. 110–116, 2010, doi: 10.1016/j.esd.2010.02.003.
- [6] M. I. Yuce and A. Muratoglu, "Hydrokinetic energy conversion systems: A technology status review," *Renew. Sustain. Energy Rev.*, vol. 43, pp. 72–82, 2015, doi: 10.1016/j.rser.2014.10.037.
- [7] S. Kelly-Richards, N. Silber-Coats, A. Crootof, D. Tecklin, and C. Bauer, "Governing the transition to renewable energy: A review of impacts and policy issues in the small hydropower boom," *Energy Policy*, vol. 101, no. November 2016, pp. 251–264, 2017, doi: 10.1016/j.enpol.2016.11.035.
- [8] F. E. Sierra, A. F. Sierra, and C. A. Guerrero, "Pequeñas y microcentrales hidroeléctricas : alternativa real de generación eléctrica .," *Inf. Técnico*, pp. 73–85, 2011.
- [9] V. Dadu, A. Dadu, D. Frunza, G. Catarig, F. Popa, and B. Popa, "Innovative Concepts Applied to Recent Small Hydropower Plants," *Energy Procedia*, vol. 112, no. October 2016, pp. 426–433, 2017, doi: 10.1016/j.egypro.2017.03.1106.
- [10] L. I. Lago, F. L. Ponta, and L. Chen, "Advances and trends in hydrokinetic turbine systems," *Energy Sustain. Dev.*, vol. 14, no. 4, pp. 287–296, 2010, doi: 10.1016/j.esd.2010.09.004.
- [11] H. J. Vermaak, K. Kusakana, and S. P. Koko, "Status of micro-hydrokinetic river technology in rural applications: A review of literature," *Renew. Sustain. Energy Rev.*, vol. 29, pp. 625–633, 2014, doi: 10.1016/j.rser.2013.08.066.
- [12] R. H. Van Els and A. C. P. B. Junior, "The Brazilian Experience with Hydrokinetic Turbines," *Energy Procedia*, vol. 75, pp. 259–264, 2015, doi: 10.1016/j.egypro.2015.07.328.
- [13] K. A. R. Ismail, T. P. Batalha, and F. A. M. Lino, "Hydrokinetic turbines for electricity generation in isolated areas in the Brazilian Amazon," *Int. J. Eng. Tech. Res.*, vol. 0869, no. 8, pp. 127–135, 2015.
- [14] R. D. Montoya Ramírez, F. I. Cuervo, and C. A. Monsalve Rico, "Technical and financial valuation of hydrokinetic power in the discharge channels of large hydropower plants in Colombia: A case study," *Renew. Energy*, vol. 99, pp. 136–147, 2016, doi: 10.1016/j.renene.2016.06.047.
- [15] D. Kumar and S. Sarkar, "A review on the technology, performance, design optimization, reliability, techno-economics and environmental impacts of hydrokinetic energy conversion systems," *Renew. Sustain. Energy Rev.*, vol. 58, pp. 796–813, 2016, doi: 10.1016/j.rser.2015.12.247.
- [16] A. H. Muñoz, L. E. Chiang, and E. A. De la Jara, "A design tool and fabrication guidelines for small low cost horizontal axis hydrokinetic turbines," *Energy Sustain. Dev.*, vol. 22, no. 1, pp. 21–33, 2014, doi: 10.1016/j.esd.2014.05.003.
- [17] Y. Yusof, "ISO 14649 (STEP-NC): New Standards for CNC Machining," *Int. J. Integr. Eng.*, vol. 2, no. 1, pp. 45–52, Jan. 2010.
- [18] A. Adam, Y. Yusof, M. Ilyas, Y. Saif, and N. Hatem, "Review on Manufacturing for Advancement of Industrial Revolution 4.0," *Int. J. Integr. Eng.*, vol. 10, no. 5, pp. 93–98, Oct. 2018, doi: 10.30880/ijie.2018.10.05.015.
- [19] R. A. Anugraha and M. R. Ibrahim, "Design and Develop of Open Architecture CNC Movement Control System for Analysing Precision Motion of EDM Machine," *Int. J. Integr. Eng.*, vol. 12, no. 3, pp. 97–106, Feb. 2020, doi: <https://doi.org/10.30880/ijie.2020.12.03.013>.

- [20] A. Ciocănea, S. Nicolaie, and C. Băbuțanu, "Reverse Engineering for the Rotor Blades of a Horizontal Axis Micro-hydrokinetic Turbine," *Energy Procedia*, vol. 112, no. October 2016, pp. 35–42, 2017, doi: 10.1016/j.egypro.2017.03.1056.
- [21] A. Lasemi, D. Xue, and P. Gu, "Recent development in CNC machining of freeform surfaces: A state-of-the-art review," *CAD Comput. Aided Des.*, vol. 42, no. 7, pp. 641–654, 2010, doi: 10.1016/j.cad.2010.04.002.
- [22] A. Z. A. Kadir, X. Xu, and F. Ridwan, "Employing Actual Shop-floor Status and Machine Tool Kinematic Data Model in Machining Simulation," *Int. J. Integr. Eng.*, vol. 3, no. 1, pp. 32–37, Sep. 2011, [Online]. Available: <https://publisher.uthm.edu.my/ojs/index.php/ijie/article/view/141>.
- [23] S.-J. Shin, J. Woo, D. B. Kim, S. Kumaraguru, and S. Rachuri, "Developing a virtual machining model to generate MTConnect machine-monitoring data from STEP-NC," *Int. J. Prod. Res.*, vol. 54, no. 15, pp. 4487–4505, Aug. 2016, doi: 10.1080/00207543.2015.1064182.
- [24] C. Danjou, J. Le Duigou, and B. Eynard, "Manufacturing knowledge management based on STEP-NC standard: a Closed-Loop Manufacturing approach," *Int. J. Comput. Integr. Manuf.*, vol. 30, no. 9, pp. 995–1009, Sep. 2017, doi: 10.1080/0951192X.2016.1268718.
- [25] W. Zhu, T. Hu, W. Luo, Y. Yang, and C. Zhang, "A STEP-based machining data model for autonomous process generation of intelligent CNC controller," *Int. J. Adv. Manuf. Technol.*, vol. 96, no. 1–4, pp. 271–285, Apr. 2018, doi: 10.1007/s00170-017-1554-9.
- [26] M. Azuddin and W. Abdullah, "A Study on Surface Roughness and Burr Formation of Al6061 with Different Spindle Speed and Federate for Small End Milling Cutter," *Int. J. Integr. Eng.*, vol. 1, no. 1, pp. 7–14, Jan. 2009, [Online]. Available: <https://publisher.uthm.edu.my/ojs/index.php/ijie/article/view/71>.
- [27] F. Ridwan and N. Xu, "Development of a surface roughness predictive model for STEP-compliant machining optimisation," *Int. J. Comput. Aided Eng. Technol.*, vol. 4, no. 3, p. 206, 2012, doi: 10.1504/IJCAET.2012.046634.
- [28] S. Abdulkareem, U. Jibrin, and A. Adaokoma, "Optimizing Machining Parameters during Turning Process," *Int. J. Integr. Eng.*, vol. 3, no. 1, pp. 23–27, Sep. 2011, [Online]. Available: <https://publisher.uthm.edu.my/ojs/index.php/ijie/article/view/116>.
- [29] M. Y. Ali, A. A. Khan, A. B. M. Asharaf, and A. A. Wahab, "Prediction of Minimum Chip Thickness in Tool Based Micro End Milling," *Int. J. Integr. Eng.*, vol. 4, no. 1, pp. 6–10, May 2012, [Online]. Available: <https://publisher.uthm.edu.my/ojs/index.php/ijie/article/view/147>.
- [30] M. Soori, B. Arezoo, and M. Habibi, "Virtual machining considering dimensional, geometrical and tool deflection errors in three-axis CNC milling machines," *J. Manuf. Syst.*, vol. 33, no. 4, pp. 498–507, 2014, doi: 10.1016/j.jmsy.2014.04.007.
- [31] W. de Oliveira Leite, J. Carlos Campos Rubio, J. Gilberto Duduch, and P. E. M. de Almeida, "Correcting geometric deviations of CNC Machine-Tools: An approach with Artificial Neural Networks," *Appl. Soft Comput. J.*, vol. 36, pp. 114–124, 2015, doi: 10.1016/j.asoc.2015.07.014.
- [32] B. Denkena, D. Dahlmann, and H. Boujnah, "Tool Deflection Control by a Sensory Spindle Slide for Milling Machine Tools," *Procedia CIRP*, vol. 62, pp. 329–334, 2017, doi: 10.1016/j.procir.2016.06.059.
- [33] C.-C. Lo, CNC machine tool surface interpolator for ball-end milling of free-form surfaces, vol. 40. 2000.
- [34] W. L. Feng, X. D. Yao, A. Azamat, and J. G. Yang, "Straightness error compensation for large CNC gantry type milling centers based on B-spline curves modeling," *Int. J. Mach. Tools Manuf.*, vol. 88, pp. 165–174, 2015, doi: 10.1016/j.ijmachtools.2014.09.006.
- [35] T. Yih-Fong and J. Ming-Der, "Dimensional quality optimisation of high-speed CNC milling process with dynamic quality characteristic," *Robot. Comput. Integr. Manuf.*, vol. 21, no. 6, pp. 506–517, 2005, doi: 10.1016/j.rcim.2004.07.014.
- [36] A. Afkhamifar, D. Antonelli, and P. Chiabert, "Variational Analysis for CNC Milling Process," *Procedia CIRP*, vol. 43, pp. 118–123, 2016, doi: 10.1016/j.procir.2016.02.164.
- [37] A. Giannakis and G. C. Vosniakos, "Parametric multi-axis tool path planning for CNC machining: the case of spur gears," *Int. J. Manuf. Res.*, vol. 7, no. 4, p. 354, 2012, doi: 10.1504/ijmr.2012.050101.
- [38] K. Schützer, E. Uhlmann, E. Del Conte, and J. Mewis, "Improvement of surface accuracy and shop floor feed rate smoothing through open CNC monitoring system and cutting simulation," *Procedia CIRP*, vol. 1, no. 1, pp. 90–95, 2012, doi: 10.1016/j.procir.2012.04.014.
- [39] M. Soori, B. Arezoo, and M. Habibi, "Dimensional and geometrical errors of three-axis CNC milling machines in a virtual machining system," *CAD Comput. Aided Des.*, vol. 45, no. 11, pp. 1306–1313, 2013, doi: 10.1016/j.cad.2013.06.002.
- [40] E. Chica, F. Pérez, A. Rubio-Clemente, and S. Agudelo, "Design of a hydrokinetic turbine," *Energy Sustain. VI*, vol. 1, no. September 2015, pp. 137–148, 2015, doi: 10.2495/esus150121.
- [41] E. Chica, F. Pérez, and A. Rubio-Clemente, Rotor structural design of a hydrokinetic turbine, vol. 11. 2016.
- [42] E. Chica and A. Rubio-Clemente, "Design of Zero Head Turbines for Power Generation," 2017.